Journal of Solid State Chemistry **158,** 320–326 (2000)
doi:10.1006/jssc.2001.9120, available online at http://www.idealibrary.com on IDEAL®

Electrical Properties of the Ferrite $SrFeO_y$ at High Temperatures

V. L. Kozhevnikov,[1] I. A. Leonidov, M. V. Patrakeev, and E. B. Mitberg

Institute of Solid State Chemistry, Ural Division of RAS, Pervomaiskaia 91, GSP-145 Ekaterinburg 620219, Russia

and

K. R. Poeppelmeier

Northwestern University, Department of Chemistry, 2145 Sheridan Road, Evanston, Illinois 60208

Received October 11, 2000; in revised form January 17, 2001; accepted February 9, 2001

The electrical properties of the strontium ferrite are reported within the temperature range 700 to 950°C and the oxygen partial pressure range between 10^{-18} and 0.3 atm. The observed pressure and temperature dependencies of the conductivity in the brownmillerite form of the ferrite are related to the transition of the electron conductivity from the intrinsic regime, which is governed by the band gap of about 2 eV, to the extrinsic regime, which is controlled by the extrastoichiometric oxygen in the brownmillerite phase. The brownmillerite phase is shown to be a mixed conductor with the oxygen conductivity rising to about 0.1 S/cm at 850–900°C and $p_{O_2} > 10^{-17}$ atm. The perovskite-like layers in the brownmillerite structure provide a possible pathway for the ion migration.

Key Words: **strontium ferrite; conductivity; thermopower; perovskite; brownmillerite; oxygen transfer.**

INTRODUCTION

The strontium ferrite $SrFeO_y$ is an inherently nonstoichiometric oxide. The oxygen deficient vacancy-ordered phases $Sr_nFe_nO_{3n-1}$, where $n = 2$, 4, 8, and ∞, are known to exist in the low-temperature range (1). At temperatures above 400°C the ferrite adopts either an oxygen vacancy disordered structure characteristic of cubic perovskite $SrFeO_{3-\delta}$ when the oxygen deficiency δ varies between 0 and 0.5, or a rhombohedral brownmillerite $SrFeO_{2.5+\delta}$ structure when the oxygen nonstoichiometry varies from -0.1 to 0.05 (2, 3). The perovskite-like form of the ferrite is a recognized mixed conductor exhibiting *p*-type, electron (4), and oxygen-ion (5, 6) components of conductivity in the high-temperature range and at sufficiently high oxygen partial pressures $p_{O_2} > 10^{-4}$ atm. The conducting properties at lower oxygen partial pressures are poorly investigated. It is known (4) that the conductivity at 800°C increases with the pressure decrease at $p_{O_2} > 10^{-13}$ atm as expected for *n*-type conductors.

The objective of the present study was therefore to measure electrical conductivity and thermopower of the ferrite in the extended range of oxygen partial pressure 10^{-18}–0.3 atm and temperature interval 700–950°C and to elucidate the mechanism of the conductivity at large oxygen deficiency.

EXPERIMENTAL

The strontium ferrite powder was made by a solid-state reaction method with appropriate amounts of high purity grade Fe_2O_3 and $SrCO_3$. Mixing and grinding of the starting reagents were carried out with addition of ethanol in a Retch laboratory mill for a period of 2 h. After drying the mixture small pellets were pressed which were then calcined in air at 900–1150°C for 70 h with intermittent grindings and pelletizations. The lower pellet served to protect the rest of the synthesized material from possible contamination by the crucible and was discarded. After the calcination, the pellets were ground in the Retch ultramill to the powder with an average grain size of about 1 μm. X-ray powder diffraction ($\lambda = 1.54178$ Å) was used to confirm the single-phase perovskite with the tetragonal elementary unit parameters $a = 10.936$ and $c = 7.709$ Å (2, 3). The powder was then pressed with a 1-kbar load into pellets 20 mm diameter and 2 mm thick. The pellets were sintered at 1200°C in air for 10 h. Densities were about 93% of theoretical. Rectangular bars $2 \times 2 \times 18$ mm were cut from the sintered pellets for electrical measurements.

The electrical measurements were carried out in a special cell made of cubically stabilized zirconia (see Fig. 1). Two pairs of platinum electrodes were deposited on the inner and

[1] To whom correspondence should be addressed. Fax: + 7-34 32-74-00-03. E-mail: kozhevnikov@imp.uran.ru.

0022-4596/01 $35.00

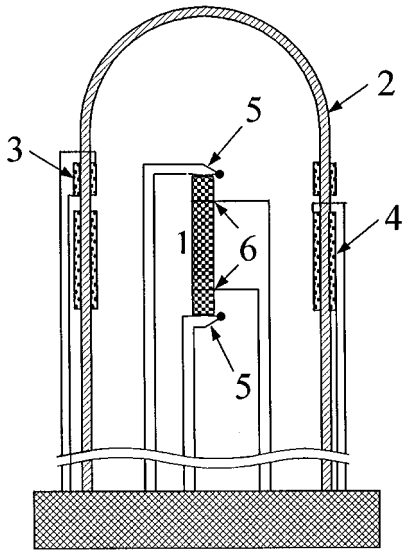

FIG. 1. Schematic drawing of the measuring cell (not on scale): 1, sample; 2, cubically stabilized zirconia; 3, sensor electrodes; 4, pump electrodes; 5, thermocouples; 6, voltage probes.

outer sides of the cell and served as the electrochemical oxygen sensor and pump. The platinum legs of Pt–Pt10Rh thermocouples were attached to the butt ends of the specimen and served as current leads or voltage probes for the simultaneous measurement of conductivity σ and thermopower α, respectively. Two additional voltage probes for the conductivity measurements were made of platinum wire and wound to the sample with an 8-mm spacing. The cell was evacuated and filled with a 50% O_2:50% CO_2 gas mixture. The cell enabled independent setting and control of the oxygen partial pressure around the specimen. A typical value of the pump current necessary to maintain the desired oxygen pressure inside the cell did not exceed 0.5 mA. The electrical parameters were measured with a precise Solartron 7081 voltmeter. A temperature gradient of 10°/cm was used in the thermopower measurements. The electrical conductivity was measured in the "true-Ω" regime, thus avoiding any influence of the thermal e.m.f on the measured values. The values of conductivity and thermopower were collected upon achievement of equilibrium between the sample and oxygen gas in the ambient. The criteria for equilibrium were selected changes in conductivity and thermopower less than 0.0005 S/min and 0.001 μV/min, respectively. The measurements were carried out in a series of isothermal experiments. Thermopower measurements were corrected for the contribution of the platinum leads (7).

RESULTS AND DISCUSSION

The isothermal plots of the logarithm of the conductivity and thermopower versus the logarithm of oxygen partial pressure are shown in Fig. 2. The complicated character of the curves reflects changes both in the oxygen content and crystalline structure of the ferrite. In the high-pressure limit, the thermopower sign is positive in accord with the earlier observed *p*-type conductivity (4). Also, the conductivity (σ) increases while thermopower simultaneously decreases with the pressure increase. Considering that $\sigma \sim p$ and $\alpha \sim \mathrm{Ln}(1/p)$, where p is concentration of electron holes, these changes indicate that the number of hole carriers increases with the pressure increase, i.e., with the increase of the oxygen content in the ferrite. This conclusion is corroborated by the Mössbauer study of $SrFeO_{3-\delta}$ (2), where it was shown that concentration of electron holes (Fe^{4+} ions) increases with oxygen content. There is a small cusp on the conductivity isotherms in the vicinity of $p_{O_2} \approx 10^{-3}$ atm, which is seen more distinctly at lower temperature. The exact position of the cusp on the pressure axis varies with temperature, i.e., it depends on oxygen content in the ferrite. As an example, the high-pressure part of the conductivity isotherm at $T = 700$°C is shown with an enlarged scale in Fig. 3 together with respective data for oxygen content (3). It was shown in work (3) that the peculiar behavior of the

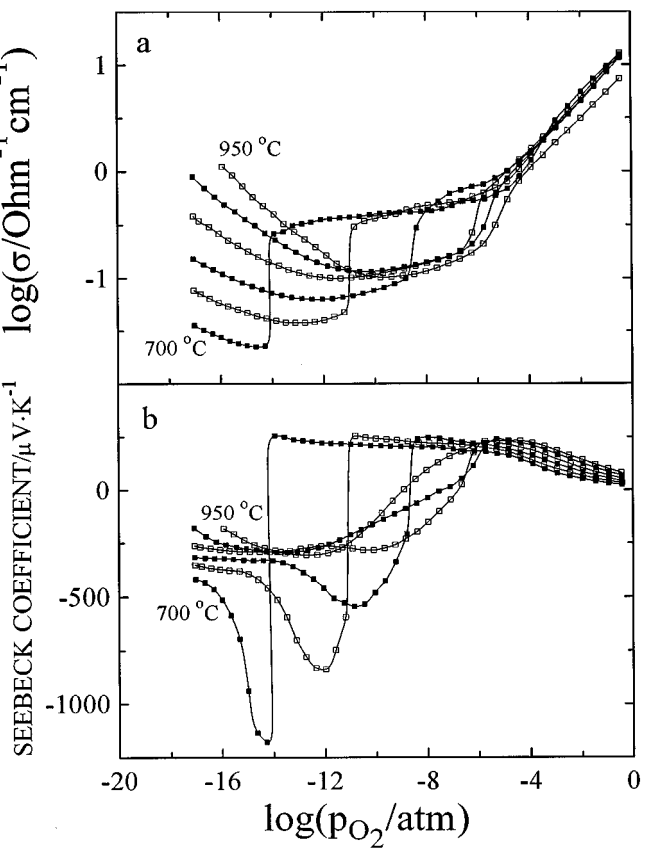

FIG. 2. The isothermal plots of the logarithm of the conductivity (a) and thermopower (b) versus the logarithm of partial pressure of oxygen. The temperature step between the isotherms is to 50°C.

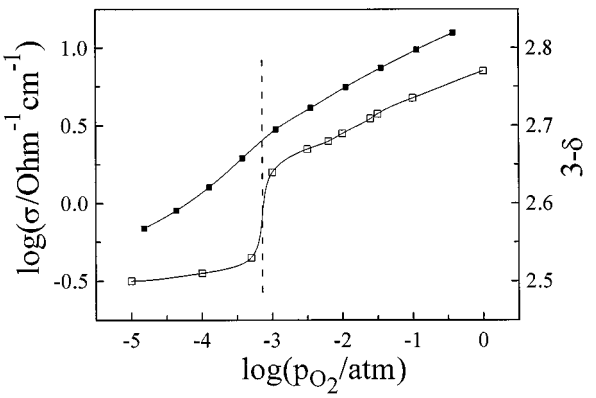

FIG. 3. The isotherms of the logarithm of the conductivity (■) and oxygen content (□) at 700°C in the range of oxygen partial pressure 10^{-5}–0.5 atm. The data for oxygen content are taken from Ref. (3). The dashed line indicates the pressure value corresponding to the perovskite to brownmillerite transition.

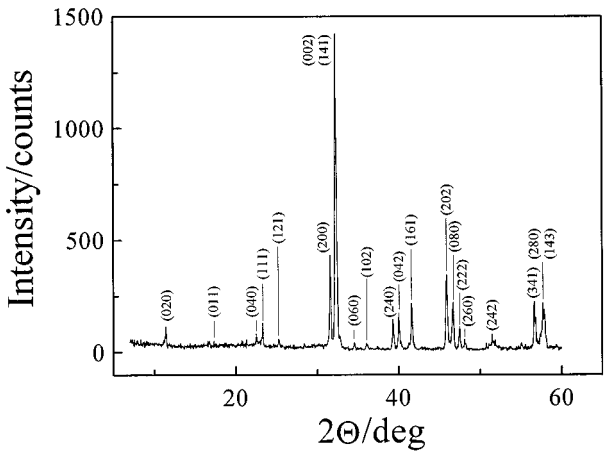

FIG. 4. The X-ray pattern of the ferrite quenched from 800°C to room temperature at $p_{o_2} = 10^{-16}$ atm. The diffraction peaks are indexed on an orthorhombic brownmillerite structure with the elementary unit parameters $a_{br} = 5.672$, $b_{br} = 15.576$, and $c_{br} = 5.528$ Å.

oxygen content corresponds to the transition of the perovskite $SrFeO_{3-\delta}$ to the brownmillerite $SrFeO_{2.5+\delta}$ structure. Therefore, the cusp is related to this transition. It is important to notice that the structural transition does not result in either the change of the sign of electronic charge carriers or a sharp change of their concentration as evidenced by thermopower. Further decrease in the pressure results in the appearance of nearly flat portions on the plots of conductivity and thermopower (see Fig. 2). X-ray diffraction patterns of the specimens quenched in a separate cell, analogous to the one depicted in Fig. 1, from the respective values of oxygen pressure and temperature confirms the brownmillerite structure. Therefore, there is a very weak pressure dependence of the oxygen content and, consequently, of the hole concentration in $SrFeO_{2.5+\delta}$ in the range of p_{o_2} and T corresponding to the flat portions. As the pressure is decreased further, both conductivity and thermopower change sharply upon achievement of some value of p_{o_2}, which depends on temperature. Although profound, these changes are not related to the decomposition of the ferrite because the quenched specimens still show the presence of the single, brownmillerite phase after the transition (see Fig. 4), based on X-ray diffraction. Therefore, the observed variations in electric properties are related mainly to changes in the electronic spectrum of the brownmillerite when the oxygen content approaches the ideal stoichiometric composition $SrFeO_{2.5}$. At even lower oxygen pressure, the conductivity isotherms have a shallow minima which then are followed by an increase in the conductivity as the p_{o_2} decreases. Hence, there are both electron σ_n and hole σ_p contributions to the conductivity. Also, very large and negative values of thermopower in the vicinity of the conductivity minima serve as evidence to polarization of the specimen and demonstrate that there is a considerable contribution of the oxygen-ion conductivity, σ_i, to the total conductivity. Therefore, the total conductivity at low p_{o_2} is given by

$$\sigma = \sigma_i + \sigma_n + \sigma_p. \qquad [1]$$

The analysis of the pressure dependencies of the conductivity results in the expected expression for a mixed, oxygen ion–electron conductor,

$$\sigma = A + B \cdot p_{o_2}^{-\frac{1}{4}} + C \cdot p_{o_2}^{-\frac{1}{4}}, \qquad [2]$$

where A, B and C are temperature-dependent parameters equal to the ion conductivity and electron and hole components of the conductivity at $p_{o_2} = 1$ atm, respectively. The values of these parameters at different temperatures were found by fitting Eq. [2] to experimental isotherms of the conductivity in Fig. 2 in the low-pressure range of the semiconductor-like behavior (Table 1). An excellent match of the isotherms calculated using these parameters and the experimental data is illustrated in Fig. 5. The temperature dependence of the obtained ion conductivity is shown in Fig. 6 with Arrhenius coordinates. The ion conductivity increases with temperature in the range 700–850°C with an activation energy equal to 1.15 eV. Similar values are observed in other perovskite-related oxides (8, 9). At higher

TABLE 1
Calculated Values for the Conductivity Parameters in $SrFeO_y$ at Different Temperatures

	700°C	750°C	800°C	850°C	900°C	950°C
A	0.014	0.028	0.051	0.084	0.090	0.057
B	1.2×10^{-6}	2.8×10^{-6}	5.8×10^{-6}	1.7×10^{-5}	4.4×10^{-5}	1.1×10^{-4}
C	17.276	9.758	7.373	5.084	4.233	4.357

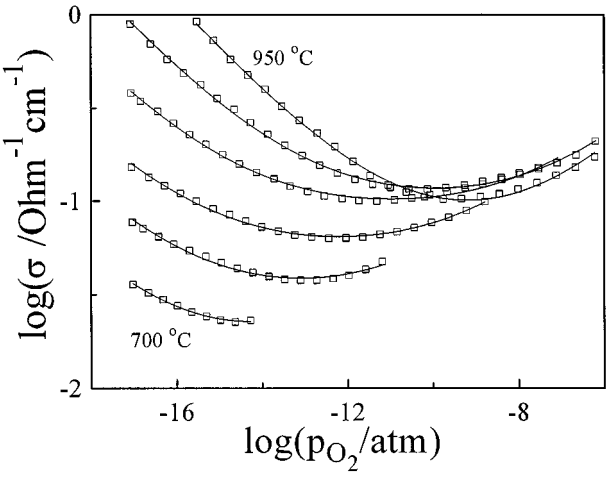

FIG. 5. Comparison of the experimental data (□) with the calculated total conductivity (lines). The temperature step between the isotherms is to 50°C.

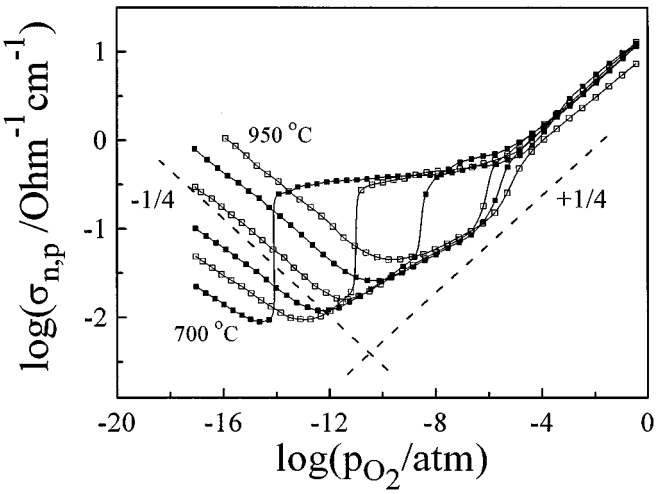

FIG. 7. The isothermal plots of the logarithm of the electron–hole contribution in conductivity versus the logarithm of oxygen partial pressure. The temperature step between the isotherms is to 50°C. The dashed lines indicate the slope of the isotherms.

temperatures, the ion conductivity decreases slightly. This decrease in σ_i explains why the total conductivity at 950°C is somewhat smaller than at 900°C in the vicinity of $p_{O_2} \sim 10^{-8}$ atm (see Figs. 2 and 5). The observed decrease in the ion conductivity may be related to partial trapping of oxygen vacancies in local clusters (e.g., $Fe'_{Fe}V''_{O}Fe'_{Fe}$), which are known in perovskite-related oxides (10, 11). Certainly, in general, an increase in temperature results in the respective increase in the total amount of oxygen vacancies and, thus, an increase in the ion conductivity. However, increasing the vacancy concentration intensifies the formation of clusters and therefore can progressively remove oxygen vacancies from the ion transfer process at sufficiently small values of p_{O_2} even when the temperature increases.

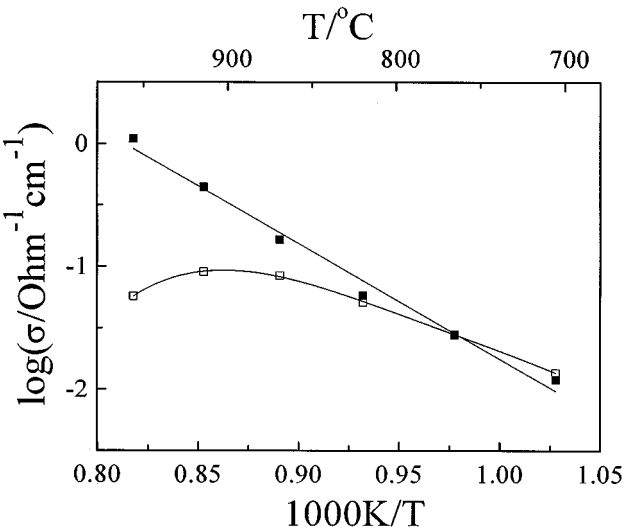

FIG. 6. The Arrhenius plots for oxygen ion (□) and electron (■) contributions in the conductivity. The data for the electron contribution (σ_n) are obtained from the isobaric cross section at $p_{O_2} = 10^{-16}$ atm in Fig. 7.

Isothermal plots of the electron–hole conductivity obtained by subtraction of the ion conductivity from the total conductivity are shown in Fig. 7. The slopes of the conductivity isotherms to the left and to the right of the minima are close to $-\frac{1}{4}$ and $+\frac{1}{4}$, respectively. The appearance of the conducting electrons in the brownmillerite form of the ferrite may be explained by the loss of lattice oxygen in the low-pressure limit,

$$O^{2-} = \tfrac{1}{2}O_2 + 2e^- \quad \text{and} \quad K_n = [e^-]^2[O^{2-}]^{-1}p_{O_2}^{\frac{1}{2}}$$
$$= K_n^0 \exp(-\Delta H_n/kT). \qquad [3]$$

Here, K_n^0 is a constant and ΔH_n is the reaction enthalpy. Hence, neglecting the mobility activation energy for electrons the proportionality $\sigma_n \sim [e^-] \sim p_{O_2}^{-\frac{1}{4}}$ follows from the equilibrium constant K_n, because the oxygen content in the brownmillerite phase depends only weakly on pressure near the stoichiometry point. Therefore, the estimated electron conductivity activation energy follows as $\Delta H_n/2$. The respective value is found equal to 2 eV (see Fig. 6) from the isobaric cross section in the *n*-type conductivity pressure range ($p_{O_2} = 10^{-16}$ atm) in Fig. 7. Thus, the enthalpy ΔH_n is equal to about 4 eV. The hole contribution, increasing with the pressure to the right of the minima, symmetrically with an increase of the electron contribution with the pressure decrease to the left of the minima in Fig. 7, is indicative of the internal equilibrium reaction,

$$0 = e^- + h^+, \qquad K_i = [e^-][h^+] = K_i^0 \exp(-E_g/kT) \qquad [4]$$

Here, K_i^0 is a constant and E_g is a band gap. The weak temperature dependence of the conductivity in the hole-like region to the right of the minima in Fig. 7 suggests a small activation energy both for the mobility and for the concentration of holes. Neglecting the mobility activation energy and combining equilibrium constants K_n and K_i, one can obtain

$$\sigma_p \sim [h^+] = \frac{K_i^0}{K_n^{0^{1/2}}[O^{2-}]^{1/2}} \exp\left(-\frac{E_g - \Delta H_n/2}{kT}\right) p_{O_2}^{-\frac{1}{4}}, \quad [5]$$

in accord with the slopes of the conductivity plots to the right of the minima in Fig. 7. Therefore, we can infer that the near equality satisfies $E_g - \Delta H_n/2 \approx 0$. Hence, the forbidden energy gap in the brownmillerite is equal to about 2 eV. The same pressure dependence of the hole contribution in the conductivity can be obtained considering directly the oxygen incorporation reaction in the stoichiometric brownmillerite

$$1/2O_2 = O^{2-} + 2h^+, \qquad K_p = \frac{[O^{2-}]}{[h^+]^2} p_{O_2}^{-\frac{1}{2}}$$

$$= K_p^0 \exp(-\Delta H_p/kT), \quad [6]$$

from which it follows that

$$\sigma_p \sim [h^+] = \frac{(K_p^0)^{1/2}}{[O^{2-}]^{1/2}} \exp\left(-\frac{\Delta H_p}{2kT}\right) p_{O_2}^{-\frac{1}{4}}. \quad [7]$$

Here, K_p^0 is a constant and ΔH_p is the reaction enthalpy. From Eq. [7], analogous to the derivation of the near equality $E_g - \Delta H_n/2 \approx 0$, we come to the conclusion that ΔH_p is close to zero also. More precisely, a weak increase in the conductivity with the temperature decrease at constant pressure right of the minima shows that ΔH_p is slightly negative. Thus, the oxygen incorporation in the brownmillerite structure is an energetically favorable reaction and is consistent with the experimental fact that the brownmillerite structure is able to tolerate some amount of extra stoichiometric oxygen (3). These results show that the concentration of electronic carriers is governed by the band gap when the oxygen content of the ferrite is close to the ideal brownmillerite stoichiometry $SrFeO_{2.5}$. Small deviations in oxygen content from the exact stoichiometry result in the shift of the intrinsic electron–hole equilibrium (Eq. [4]) and the prevalence of either electrons or holes contributing to the conductivity and negative or positive values of thermopower with the loss or uptake of oxygen, respectively. Strictly speaking, the minima of the conductivity isotherms must be exactly at oxygen pressure values corresponding to zero thermopowers while, in fact, the thermopower zeros are located at slightly higher pressures. This small and decreasing with increasing temperature displacement is related to the specimen polarization because of the ionic contribution as explained above. At increasing pressure of oxygen and decreasing temperature the flat portions on the conductivity plots appear. This change can be interpreted as an indication that the conductivity acquires an impurity-controlled character, i.e., becomes governed by the amount of extrastoichiometric oxygen δ in $SrFeO_{2.5+\delta}$. In other words, impurity-like, acceptor states appear above the top of the valence band upon incorporation of some small but critical amount of extrastoichiometric oxygen in the brownmillerite structure. The energy spacing between the impurity states and the top of the valence band should be about 0.1 eV or smaller for all acceptors to be fully ionized at the characteristic temperature of the experiment (~ 1000 K). Consequently, the electron conductivity on the flat portions of the isotherms in Fig. 7 is governed only by the concentration of the "extra" oxygen incorporated in the brownmillerite structure. It is interesting to notice that the increasing oxygen content in the brownmillerite results in a smooth increase of the conductivity, and the transition of the brownmillerite structure to the perovskite one is accompanied by only minor changes in conductivity. This demonstrates that the impurity-controlled regime of the conductivity persists at the higher oxygen content, but the impurity states form a band that merges with the valence band. From this viewpoint, the electronic properties of the perovskite $SrFeO_3$ correspond to the properties of the oxide matrix $SrFeO_{2.5}$ heavily doped with oxygen (see Fig. 8). The left-hand side of the figure depicts a proposed band scheme for the near stoichiometric brownmillerite whereby oxygen depletion/uptake leads to small upward or downward shifts of the Fermi level from the near mid-gap position and dominance of negative or positive carriers, respectively. Incorporation of a sufficiently large amount of oxygen in the brownmillerite $SrFeO_{2.5+\delta}$ results in the appearance of impurity-like,

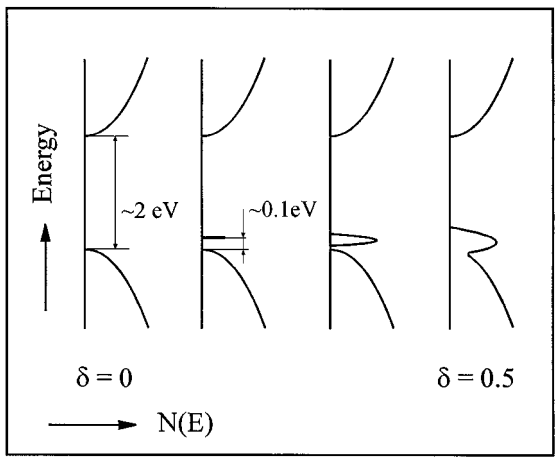

FIG. 8. A schematic drawing of the proposed changes in the density of electron states $N(E)$ in the ferrite $SrFeO_{2.5+\delta}$ at transition from stoichiometric brownmillerite $\delta = 0$ to perovskite $\delta = 0.5$. The drawings from left to right correspond to increasing oxygen content.

acceptor states and a strong shift of the Fermi level to the position between the impurity states and the top of the valence band when there is the impurity-controlled conductivity. Further oxygen intake, up to the perovskite composition $SrFeO_3$, results in broadening of the array of the acceptor states and closing of the gap separating them and the valence band, as is shown on the right-hand side of Fig. 8, while the Fermi level is now at the top of the presumably broad valence band, thus rendering enhanced hole conductivity. The model relates the impurity levels and electron states of the oxygen incorporated in the structure and essential *p*-character of electron holes. Such a conclusion is supported by recent electron energy loss studies in the solid solution $SrTi_{1-x}Fe_xO_{3-\delta}$ (12) and by Mössbauer measurements for oxygen vacancy ordered ferrites $Sr_nFe_nO_{3n-1}$ (1).

It is seen from Fig. 6 that the oxygen ion conductivity in the brownmillerite phase achieves values of about 0.1 S/cm at 850–900°C, which is comparable with the ion conductivity of electrolytes based on YSZ (13) and $LaGaO_3$ (14). Nonetheless, this value is smaller than $\sigma_i = 0.035$ S/cm found in the perovskite phase $SrFeO_{3-\delta}$ from permeation data at 850°C (5). This difference in the ion conductivity appears quite natural considering the difference in the two crystalline modifications of the ferrite. As a rough approximation, all oxygen ions participate in the conduction, while almost all oxygen vacancies are disordered and, thus, equally available for a jump site for the oxygen ions in the perovskite phase. Both factors contribute to the high level of the conductivity. In contrast, the oxygen vacancies are ordered in the brownmillerite phase, creating layers of iron–oxygen tetrahedra separated by layers of the vacancy free iron–oxygen octahedra, see Fig. 9. This ordering phenomenon usually greatly reduces the ion conductivity in brownmillerite type metal oxides. For example, the oxygen conductivity of $CaFeO_{2.5}$ does not exceed 0.001 S/cm at 950°C (15). $SrFeO_{2.5}$ is peculiar because the large size of the Sr^{2+} ion results in only small differences in the pseudocubic perovskite lattice parameters with $a_{br}/\sqrt{2} \approx b_{br}/4 \approx c_{br}/\sqrt{2}$ (2). Therefore, some fraction of oxygen ions in the iron–oxygen octahedra can leave their regular positions and fill structural vacancies in the layers of iron–oxygen tetrahedra in $SrFeO_{2.5+\delta}$. This anti-Frenkel disordering reaction may be written as

$$V_{O,tet} + O_{oct}^{2-} = O_{tet}^{2-} + V_{O,oct}, \qquad [8]$$

where $V_{O,tet}$ and $V_{O,oct}$ denote vacant oxygen positions in the iron–oxygen tetrahedra and octahedra, respectively. Two pathways for oxygen migration can be envisioned. One is related to movement of the interstitial oxygen over the structural vacancies that form one-dimensional tunnels in the layers of tetrahedra, while the second involves oxygen ion jumps over a two-dimensional network of vacancies in the layers of octahedra. The activation energy for ion jumps in the layers of iron–oxygen tetrahedra may be smaller than for the jumps in the layers of octahedra. However, the product of the redistributed oxygen concentration δ_r by the vacancy concentration $(2 - \delta_r)$, which defines the jump availability, is larger in the layers of octahedra than the respective value $\delta_r(1 - \delta_r)$ in the layers of tetrahedra. Also, extended defects such as dislocations and grain boundaries, which inevitably are present in the polycrystalline material, greatly reduce the one-dimensional oxygen transfer. Therefore, the perovskite-like layers would appear to provide a viable pathway for oxygen migration in the brownmillerite modification of the ferrite.

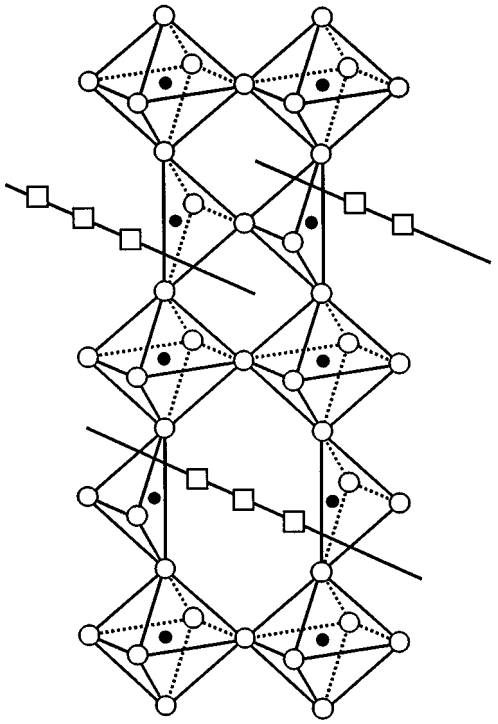

FIG. 9. A sketch of the brownmillerite structure showing alternating layers of the iron–oxygen octahedra and layers of the iron–oxygen tetrahedra with tunnels formed by ordered oxygen vacancies. ●, Iron ion; ○, oxygen ion; □, oxygen vacancy.

CONCLUSIONS

The electrical conductivity and thermopower of the strontium ferrite were measured in the temperature range 700–950°C and oxygen pressure varying between 10^{-18} and 0.3 atm. Decreasing the oxygen pressure results in the transition of the perovskite to the brownmillerite structure below about 10^{-3} atm. The brownmillerite form of the ferrite is shown to be a mixed conductor with the oxygen conductivity increasing to about 0.1 S/cm at 850–900°C and $p_{O_2} > 10^{-17}$ atm. The calculated oxygen flux from a 1-mm ceramic membrane with $p_{O_2}^{high}/p_{O_2}^{low} = 0.21$ atm/10^{-16} atm is

estimated to be about $3\,ml/cm^2 \cdot min$. It is argued that the oxygen conduction takes place mainly in the perovskite-like layers of the brownmillerite structure. The electron–hole conductivity in the near stoichiometric brownmillerite phase is shown to be governed by the band gap of about 2 eV. Increasing the extrastoichiometry oxygen in the brownmillerite results in the appearance of acceptor states above the top of the valence band and marks the transition of the conductivity to an impurity-controlled regime.

ACKNOWLEDGMENTS

We acknowledge partial support of this work by the Russian Foundation for Basic Research under Award 98-03-3251a. One of us (K.R.P.) is grateful to the EMSI program of the National Science Foundation and the U.S. Department of Energy Office of Science (CHE-9810378) at the Northwestern University Institute for Environmental Catalysis.

REFERENCES

1. J. P. Hodges, S. Short, J. D. Jorgensen, X. Xiong, B. Dabrowski, S. M. Mini, and C. W. Kimball, *J. Solid State Chem.* **151,** 190–209 (2000), doi:10.1006/jssc.1999.8640.
2. Y. Takeda, K. Kanno, T. Takada, O. Yamamoto, M. Takano, N. Nakayama, and Y. Bando, *J. Solid State Chem.* **63,** 237–249 (1986).
3. J. Mizusaki, M. Okaysu, S. Yamauchi, and K. Fueki, *J. Solid State Chem.* **99,** 166–172 (1992).
4. F. W. Poulsen, G. Lauvstad, and R. Tunold, *Solid State Ionics* **72,** 47–53 (1994).
5. Y. Teraoka, H.-M. Zhang, S. Furukawa, and N. Yamazoe, *Chem. Lett.* 1743–1746 (1985).
6. A. Holt, T. Norby, and R. Glenne, *Ionics* **5,** 434–443 (1999).
7. N. Cusak and P. Kendall, *Proc. Phys. Soc.* **72,** 898–901 (1958).
8. J. Mizusaki, *Solid State Ionics* **52,** 79–91 (1992).
9. H. Iwahara, T. Esaka, and T. Mongahara, *J. Appl. Electrochem.* **18,** 173–177 (1988).
10. J. A. M. van Roosmalen and E. H. P. Cordfunke, *J. Solid State Chem.* **93,** 212–219 (1991).
11. M. V. Patrakeev, I. A. Leonidov, E. B. Mitberg, A. A. Lakhtin, V. G. Vasiliev, V. L. Kozhevnikov, and K. R. Poeppelmeier, *Ionics* **5,** 444–449 (1999).
12. S. Steinsvik, R. Bugge, J. Gjønnes, J. Taftø, and T. Norby, *J. Phys. Chem. Solids* **58,** 969–976 (1997).
13. J. C. Boivin and G. Mairesse, *Chem. Mater.* **10,** 2870–2888 (1998).
14. T. Ishihara, H. Matsuda, and Y. Takita, *Solid State Ionics* **79,** 147–151 (1995).
15. M. V. Patrakeev, E. B. Mitberg, I. A. Leonidov, and V. L. Kozhevnikov, unpublished results.